Received: 9 November 2023 | Revised: 23 November 2023 | Accepted: 29 November 2023

DOI: 10.1002/pls2.10114

RESEARCH ARTICLE

SPE POLYMERS WILEY

A designer Schiff based motif offered dual dynamic exchangeable bonds, faster curing and closed-loop circularity in epoxy vitrimers

Sandeep Tripathi | **Supriya H.** | **Suryasarathi Bose**

Department of Materials Engineering, Indian Institute of Science, Bengaluru, India

Correspondence
Suryasarathi Bose, Department of Materials Engineering, Indian Institute of Science, Bengaluru 560012, India.
Email: sbose@iisc.ac.in

Abstract

A fast-curing epoxy with improved mechanical properties, self-healing and re-processability was designed using a tailored Schiff based motif that offered dual covalent adaptable network (CAN) in epoxy. The designer motif is a dynamic hardener with both acetal linkage and a Schiff base motif in the same molecule which allowed us to gain a mechanistic insight into the evolving transient network in epoxy vitrimers. The dynamic hardener besides offering a cross-linked network in epoxy can facilitate rapid exchange reactions, resulting in a material with high tensile strength (74 MPa), high glass transition temperature (121°C), and that can be re-purposed through solvent induced degradation. The proposed dynamic curing agent is suitable to be employed as a coating material on substrates to ensure excellent self-healing and re-processability ensuring chemical recyclability. Few carbon fiber-based laminates were prepared using the epoxy vitrimer and the recovery of CF post laminate preparation clearly demonstrates the closed-loop circularity in epoxy vitrimers.

Highlights

- A unique dynamic curing agent is designed consisting of an aldehyde (salicylaldehyde) and an amine and acetal containing species (amino acetaldehyde dimethyl acetal).
- It facilitates imine and acetal exchange that can bond at temperatures <60°C and break at temperatures >105°C as evidenced by the vitrimer transition temperature.
- Epoxies show high tensile strength (74 MPa), exceptional Tg (121°C), fast stress relaxation and an activation energy of 96.2 KJ/mol.
- The imine-acetal exchange system rendered the epoxies re-processable, malleable and re-usable.

KEYWORDS

amino acetaldehyde dimethyl acetal, CAN's, recyclable, reprocessing, reshaping, reusable, salicylaldehyde

Sandeep Tripathi and Supriya H. contributed equally to this work.

1 | INTRODUCTION

The term "plastic" refers to all synthetic materials utilized in household and packaging articles based on the requirements of one's lifestyle, it can be re-molded and adapted into applications. They are ideal materials for modern applications with a low ecological footprint due to their low cost, lightweight, high performance, ease of production, overall durability, and adaptability.[1] Due to the dimensional stability, chemical inertia, and temperature-dependent rigidity, thermoset elastomers such as vulcanized rubber are dependable materials for a wide range of applications.[2] On heating, these soft, viscous polymers undergo extensive crosslinking, resulting in insoluble, hard, and irreversible products. The lack of malleability and covalent permanent linkages limits their recycling and results in a lot of waste and may eventually end up in landfills and pollute the environment. On the contrary, the rubbery nature and low glass transition temperature (Tg) of thermoplastic elastomers allow for significant mechanical deformation and extension. There is a loss of chemical resistance and dimensional stability at elevated temperatures due to the absence of crosslinking junctions, but an excellent advantage to stretchability and re-processability.[3] The new improvements in polymer science helps with obscuring the lines among thermoplastic and thermosets for improvement of polymeric elastomers that have a consolidated favorable property of both, for example, improved mechanical strength, chemical and thermal stability, re-processability, and the ability to rearrange network topologies in response to stimuli (such as light or temperature). The development of materials known as vitrimers, which offer superior advantages, is aided by the incorporation of dynamic covalent networks. These dynamic covalent networks serve as a transition between thermosets and thermoplastics, assisting in providing excellent thermomechanical stability as observed in thermosets and malleability and re-processability as seen in thermoplastics.[2]

As the material's temperature falls below the Tg, it behaves like a solid exhibiting an elastic modulus of 10^9 to 10^{10} Pa.[4] Metal–ligand coordination, hydrogen bonding, and ionic interaction are examples of reversible non-covalent interactions that cannot withstand massive stress and have poor mechanical properties, making them unsuitable for structural applications.[5] Reversible, covalent adaptable networks (CANs) typically aid in the creation of materials with superior tensile strength properties. The inherent exchangeable covalent linkages naturally assist in flow, mobility and bond exchange for self-healing and shape memory ability.[6,7] Covalent networks can be divided into two categories based on crosslink exchange mechanism: associative and dissociative. Similar to the S_N2 reaction, the associative (miscellaneous) reaction begins with the formation of new bonds before the bond breaks, whereas the dissociative reaction begins with the bond breaking before the bond reforms, like the S_N1 reaction. Dissociative CANs have bonds that dissolve when they break in the solid state, are unlikely to reform, swell and lose their integrity, whereas associative CANs have constant crosslinking density and exhibit superior resistance to non-reactive solvents.[8] Associative CANs conserve the crosslinking density throughout dynamic exchange and result in short-lived intermediates that spontaneously fragment to restore the network to the same chemical functionality but with different connectivity. The time-dependent behavior of associative CANs is solely dependent on the reaction kinetics, which are tunable by the chosen catalyst and the relative concentrations of the reactive species. But when the equilibrium thermodynamics are shifted, typically through the application of a stimulus such as heating, dissociative CANs employ chemical reaction equilibria in which the reaction products, resulting in crosslinks, revert to the reactants. Consequently, if the equilibrium conversion to adducts is sufficiently reduced, the polymer network will revert to low-viscosity monomers.[9] Few studies have been carried out on dissociative CANs such as furan maleimide Diels Alder, thioacetal exchange, amine urea exchange, and transcarbamylation of urethanes.[10] Likewise, reversible miscellaneous adaptable networks were designed as observed in transesterification,[11–13] transcarbamoylation,[14] vinylogous urethane,[15,16] boronic ester metathesis,[17,18] Silyl ether,[19,20] disulfide metathesis,[21–23] imine,[24–26] thioether,[27] acetal exchange,[28,29] and so on. The malleability and recyclability of acetal dynamic covalent networks were outstanding. They demonstrated quick stress relaxation at higher temperatures.[28] The acetal bond is involved either in acetal metathesis polymerization (AMP), which eliminates the acetal ROCH2OR, or transacetalization with an alcohol chain end, which eliminates the alcohol ROH. The first procedure technically does not include metathesis because it involves two distinct functional groupings.[30] Hence, acetal dynamic linkage will enhance acetal chemistry and provide a novel route for the creation of dynamic covalent networks without the need for catalysts.

Epoxy resins are widely used for the fabrication of adhesives, coatings and in the creation of composites due to their ease of handling, processability, excellent solvent resistance, dimensional stability, and resistance to corrosion.[31,32] High-performance lightweight composite materials are of great interest due to their outstanding mechanical and thermal properties. Employing epoxy resins as the matrix for composites require

material with low thermal expansion coefficient, high heat and moisture stability[31,33] and these parameters can be achieved through modifications in the pendant and backbone groups and the highly cross-linked three-dimensional networks in epoxy amine blends exhibit high mechanical properties and is an exceptional adhesive.[32] However, epoxy curing with amine results in a non-reversible reaction, and the matrix does not produce depolymerization products, thus failing the recycling strategy. To this end, several CANs as mentioned have been installed to design vitrimer however, a mechanistic insight as to how a designer molecule can be tweaked to harness both single and dual CANs and its effect on the structure–property correlation is not fully understood. It should be emphasized that EP vitrimers with a single-dynamic covalent network face the challenge of having to satisfy both good mechanical capabilities and self-healing qualities or recyclability. Mechanical qualities are primarily determined by the stiff structure and cross-linking density of EP, whereas self-healing capabilities or recyclability are determined by the concentration of reversible covalent bonds. Unfortunately, adding too many reversible covalent bonds to the EP vitrimer would degrade its mechanical properties.[34]

Current research has focused on the formulation of epoxy vitrimers by employing dual dynamic systems and the study of vitrimer dynamic properties by adding disulfide-imine systems (from vanillin- AFD curing agent) exhibited good solvent resistance and good tensile strength.[34] Similarly, as a curing agent, terephthaldehyde and 4-AFD were employed to supply the disulfide and imine linkages to make epoxy vitrimer, which can be chemically reprocessed to provide sustainability.[35] Until now, no research has been established that uses acetal as one of the motifs for the formulation of dual dynamic curing agent, and this innovative way is studied here to obtain an epoxy vitrimer with outstanding tensile strength (75 MPa) and self-healing ability.

Hence, to endow the ability of reprocessing, recycling, and self-healing, a dual CAN with the same Schiff based motif has been installed into the traditional epoxy here. This Schiff base motif containing both acetal and imine exchangeable groups will pave the way for a cross-linked structure through the dynamic exchangeable bonds and enables the material to switch between thermoset and thermoplastic beyond a certain temperature. The designer Schiff based motif allows trans-acetalization, where a hydroxyl group reacts with an acetal, displacing part of it to form a new acetal, acetal exchange and in addition, acetal metathesis-triggered by heat.

2 | EXPERIMENTAL SECTION

2.1 | Materials and methods

The diglycidyl ether of bisphenol (DGEBA) with an epoxy equivalent weight (g/eq) range of 169–185 was obtained from Atul Ltd. India. Additionally, the epoxy resin (EP- Lapox ARL-135LV) and the amine-based hardener (Lapox AH-411) were purchased from the same source. Amino acetaldehyde dimethyl acetal, salicylaldehyde, and 1-(3-aminopropyl) imidazole (API) were procured from Sigma Aldrich. The solvents NMP (from Spectrochem PVT.LTD Mumbai, India), DMSO (from SDFCL), DCM, acetone, ethyl acetate (from FINAR), and ethanol (from Sigma Aldrich) were also acquired. Sodium hydroxide and sodium sulfate were obtained from SDFCL. All chemicals used were of analytical grade and used as procured.

2.2 | Synthesis of an imine-acetal based hardener employing naturally occurring compounds

Amino acetaldehyde dimethyl acetal (A^2—30 mmol) was combined with salicylaldehyde (S—30 mmol) to design a Schiff base, denoted as A^2S by employing ethanol as the solvent. Carbonyl group in salicylaldehyde behaves as an electrophile and is involved in an addition reaction with the primary amine (nucleophile) of A^2 as illustrated in Figure 1A,C. The reactants were introduced into a round bottom flask containing 100 mL ethanol and was further equipped with a reflux condenser. The contents in the flask were agitated continuously by simultaneously heating at 65°C for 3 h as depicted in Figure 1B. Rotary evaporation was employed to recover the solvent ethanol from the contents to obtain a yellow solution. The obtained crude product was recrystallized employing ethyl acetate to obtain the Schiff's base (A^2S) in 90% yield. The purified sample is stored for further use.

2.3 | Fabrication of dual dynamic vitrimer of A^2S

The Schiff base moiety A^2S synthesized in Section 2.2 was combined in 10, 20, and 30 wt% of epoxies in combination with accelerator API (2.4 mol%) by a one-step procedure. Pre-curing of epoxy was carried out by employing different concentrations (10%, 20%, and 30%) of A^2S following a curing time ranging from 1 to 2 h. A detailed description containing the different compositions and curing cycle and time is tabulated in Table S1.

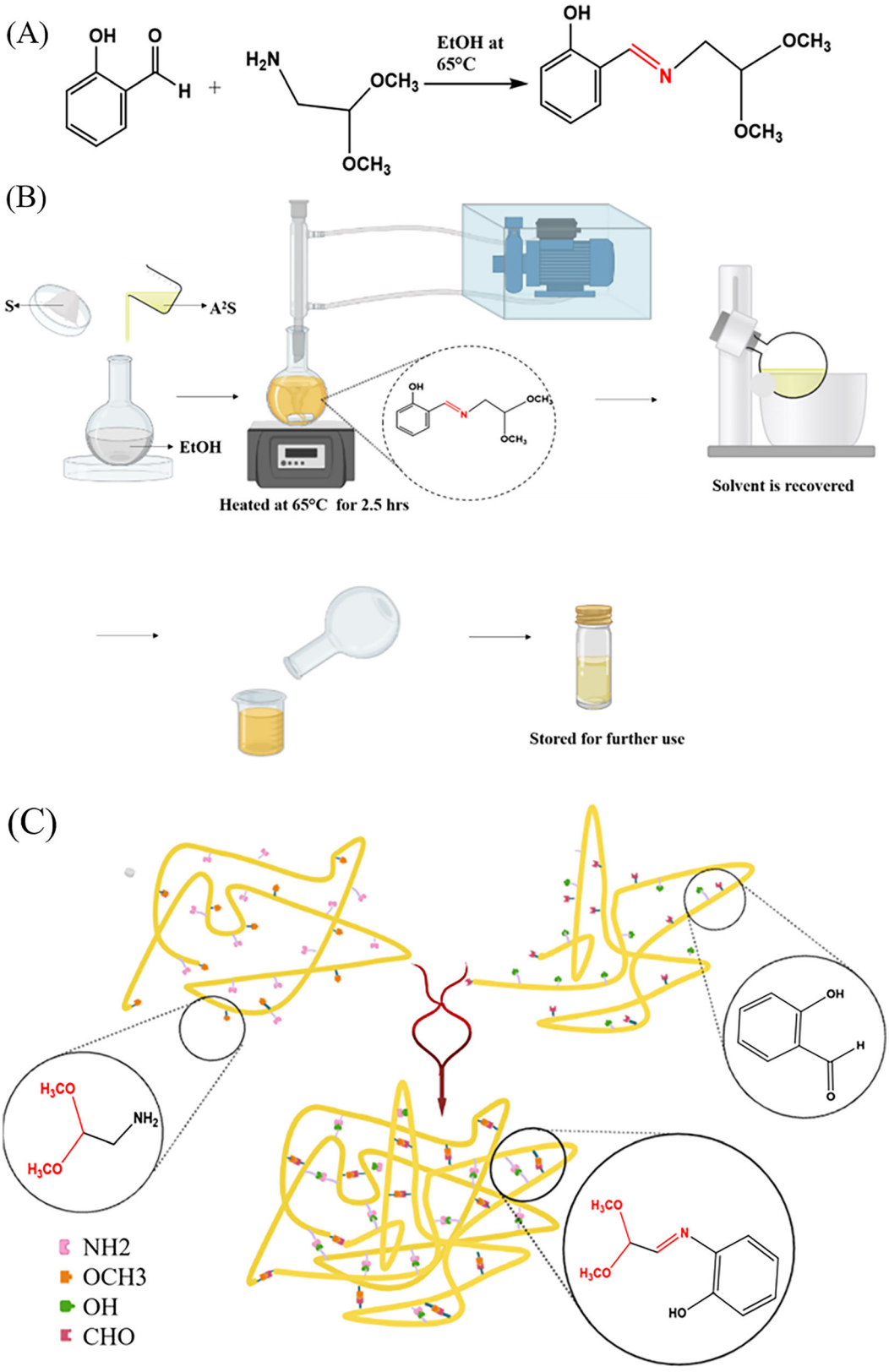

FIGURE 1 (A) The synthesis route of formation of A^2S; (B) A schematic illustrating the sequential steps employed to obtain the crude product; (C) Graphical illustration of the acetal and Schiff base linkage formed.

Following this, accelerator API was added to the reaction mixture and stirred. The resulting mixture was degassed for 10–15 min and transferred into a preheated mold to cure the samples following a heat profile—120°C for 1 and 2 h by placing it in a hot air oven. Employing A^2S in 10 wt% of epoxy and cured in 1 h yielded a sample

which is denoted as A^2S_10%_1 h. Likewise, samples cured with alternate wt% and time are tabulated in Table S1.

The mechanism followed by the inherent hydroxyl group of the hardener A^2S in assisting the ring opening of the epoxy group of the resin DGEBA employed via a S_N2 addition is illustrated in Figure 2A. The reversible covalent adaptive networks of the designed dual dynamic vitrimer—acetal exchange and imine exchange that transpire in the presence of heat is depicted in Figure 2B. The mechanism involved with the catalyst, hardener and epoxy for successful curing and establishment of superior properties is illustrated in Figure S1.

2.4 | Fabrication and investigation of dual dynamic vitrimer coating

The designed vitrimer is employed in fabricating a coating that encompasses all the advantages that is bestowed by the dynamic exchange networks of A^2S. The pre-cured sample Ep-A^2S_20% was coated on glass, PET, metal, and carbon fiber as shown in Figure S2 and subjected to investigations as mentioned further to establish the self-healing ability, re-processability and recycling ability endowed by the dual reversible bonds. To determine the substrate's recyclability, the coating on the glass slide was submerged in a glass beaker containing 1 N HCl: THF solution. A scratch was mechanically induced on a coated glass substrate as developed and was heated at 150°C for 2 h. Carbon fiber recovery from carbon fiber reinforced vitrimer was demonstrated by immersing a portion of carbon fiber coated with the dual dynamic vitrimer in a solution of 1 N HCl and THF (1:1) for 24 h at 100°C to obtain a neat fiber still maintaining its integrity.

2.5 | Reprocessing ability of the A^2S cured epoxy

Mechanical re-processability of the samples fabricated following Section 2.3 are demonstrated by crushing into smaller chunks using a mortar and pestle. The obtained chunks were further powdered using a mixer and the fine powder obtained was carefully packed into a rectangular teflon-coated mold and subjected to compression molding at a pressure of 5 MPa and temperature of 185°C for 3 h. The samples are cooled and demolded to obtain reprocessed epoxy vitrimer maintaining its integrity as depicted in Figure 9A. Likewise, effective chemical recyclability of the samples was demonstrated by investigating the network stability of the samples by conducting the swelling and solubility tests as demonstrated in Figures S4 and S5. The swelling ratio and soluble fraction tests obtained reveals the intensity of crosslinks developed in the system. A piece of designed sample with a weight of about 50–60 mg was measured and submerged

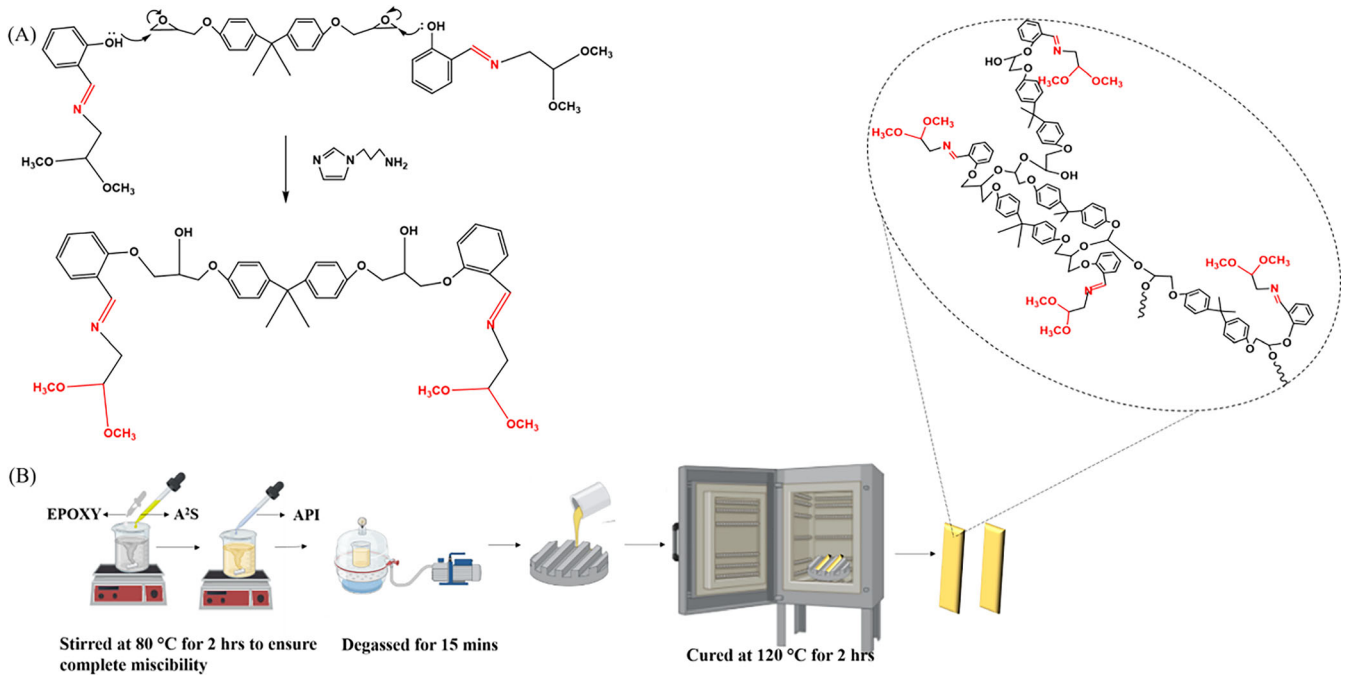

FIGURE 2 (A) Representation of the chemical reaction occurring between DGEBA and the designed hardener A^2S; (B) The depiction of the thermo-reversible exchange network functioning in the system along with curing steps involved.

in 5 mL of acetone for 24 h at room temperature. The material was further reweighed to assess the degree of swelling after the swelling had taken place and tabulated in Table 1. The following formula was used to determine the swelling ratio:

$$\text{Swelling ratio}\,(\%) = \frac{m_1 - m_2}{m_2} \text{x}\,100, \quad (1)$$

m_1 is the initial mass and m_2 is the enlarged mass.

Approximately 95–130 mg of a different, smaller piece of the processed sample was weighed and heated at 150°C for 24 h in a solution containing NMP and DMSO in a 1:1 ratio. The sample was then reweighed after drying under vacuum for a further 2–3 days at 95°C. The following formula was used to determine the soluble fraction:

$$\text{Soluble fraction}\,(\%) = \frac{m_i - m_d}{m_i} \text{x}\,100, \quad (2)$$

m_i is the initial mass and m_d is the enlarged mass.

Further, the self-healing potential of the designed vitrimer was investigated by scratch healing test. A scratch was mechanically induced on a coated glass substrate and placed in an oven for 2 h at 150°C. The healing of the scratch was monitored and recorded as depicted further.

2.6 | Characterization

The fabricated samples were subjected to Fourier transform Infrared spectroscopy, ^{1}H NMR, TGA, DSC, Shore D hardness, Tensile and dynamic mechanical analysis and the specifications of the preparation of samples and instruments are mentioned in Data S1.

3 | RESULTS AND DISCUSSION

The concentration of the designer dynamic hardener (A^2S) was varied here (10, 20, and 30 wt%) to optimize the loading, but concentrations above 20% caused problems with processability. When the epoxy was cured using 10% hardener, samples were only partially cured even after 2 h. The optimum hardener concentration was observed to be 20% based on spectroscopic evidence and the thermomechanical properties. Crosslinking is possibly impeded due to higher steric hindrance at higher hardener concentrations, resulting in a more tangled network and increased chain stiffness. Epoxy resins with phenol groups have low cure reactivity, so hardener accelerators like API are needed to speed up reaction kinetics and reduce the activation energy of the system.

3.1 | Designer dynamic hardener with dual CANs

A system containing two exchange networks- acetal and imine is designed by initially combining an acetal and amine containing moiety (A^2) with an aldehyde and hydroxyl group containing moiety (S) to obtain A^2S and the progress and the completion of reaction was mapped by recording the FTIR spectra as depicted in Figure 3A. The C—O stretching and C—H stretching at 1128 and 2900 cm^{-1}, respectively is observed as it is embedded in A^2 and post reaction with S, the C—N stretch at 1694 cm^{-1} confirms the formation of imine linkage. Moreover, the absence of carbonyl stretching C═O for aldehydes at 1740–1720 cm^{-1} confirms the formation of Schiff base motif. Based on this information, we fixed the concentrations of the hardener (20%) and cured the vitrimers at different times and systematically investigated using FTIR to confirm the complete conversion of the epoxy groups. The absence of oxirane peak and the appearance of aliphatic C—O—C signal at 1180 cm^{-1} following the ring opening of epoxy by the hydroxyl groups (see Figure 3B) confirmed the curing of the epoxy vitrimers. The opening of an epoxy ring can occur by two mechanisms: (a) by hydroxyl moiety embedded in the synthesized hardener A^2S as depicted in Figure S1a; (b) in the presence of imidazole moiety[36] as depicted in Figure S1b. This can be clearly distinguished

TABLE 1 The data obtained during swelling and solubility test.

Samples	Initial mass (mg)	Swollen mass (mg)	Swelling ratio (%)	Initial mass (mg)	Soluble mass (mg)	Soluble fraction (%)
A^2S_10%_2 h	55.4	57.5	3.8	109.7	95.9	14.39
A^2S_20%_2 h	54.5	55.7	2.2	117.8	96.2	22.45
A^2S_30%_2 h	56.4	60.8	7.8	129.0	95.7	34.79

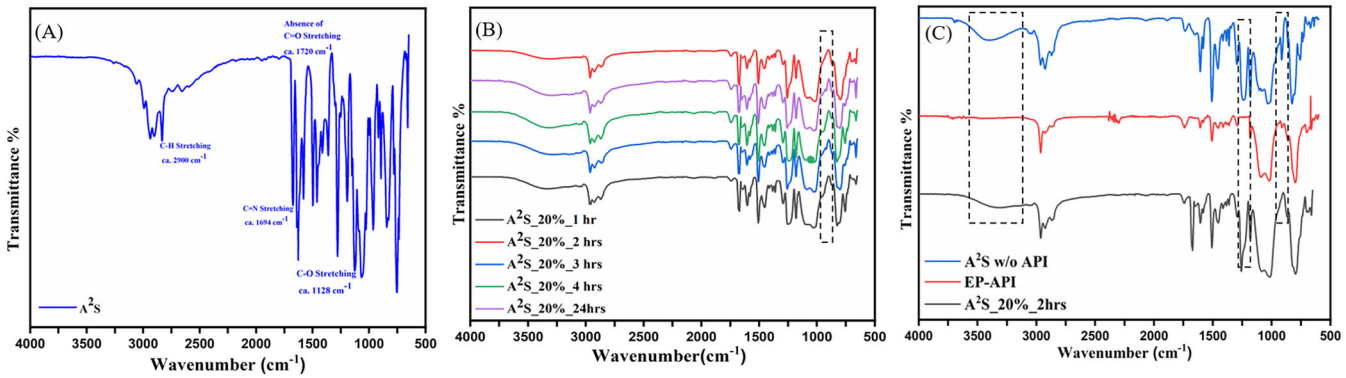

FIGURE 3 (A) FTIR spectra of A^2S; (B) FTIR of cured epoxy samples employing different concentrations and curing times with A^2S.

by comparing the FTIR spectra as depicted in Figure 3C. It can be observed that in the case of EP-API, incomplete curing is confirmed by the presence of oxirane peak at 911 cm^{-1} and the polyether formation, via the homopolymerization of the epoxide, is observed in the presence of API which is indicated by the aliphatic C—O—C signal at 1180 cm^{-1}, but there is absence of broad peak in the range of 3400–3300 cm^{-1} whereas in the case of A^2S_20%_2 h, upon curing, the complete curing is confirmed by the absence of oxirane peak at 911 cm^{-1} and there is presence of hydroxyl peak in the range of 3400–3300 cm^{-1} generated by the opening of epoxide in DGEBA confirming that the complete curing is assisted by the hydroxyl groups inherent in hardener A^2S. Further, ether peak is observed in the samples cured with A^2S in the range of 1250–1230 cm^{-1} which further confirms the ring opening of the epoxy ring. The homopolymerization of epoxy by API also shows that. Figure 3C also depicts the presence of oxirane peak 911 cm^{-1} in the sample A^2S_20%_w/o-catalyst which confirms the incomplete curing of the sample in the absence of a catalyst.

As characterized by FTIR, complete curing of the samples were observed within 2 h and this was assisted by the combined activity of the accelerator API and hardener A^2S.

The coupling product derived by reacting salicylaldehyde and amino acetaldehyde dimethyl acetal was used to synthesize imine and the confirmation of the successful formation of the Schiff base motif can be confirmed by the ^{1}H-NMR spectrum in Figure 4. The multiple peaks appearing at the chemical shifts of 6.9–7.5 ppm could be assigned to aromatic protons. The sharp peak appeared at 9.9 ppm due to the resonance of the aldehyde proton being completely absent confirms successful condensation of aldehyde and amine to form imine as observed at a chemical shift. The sharp peak that is shown at the chemical shift 13.43 ppm could be assigned to the proton of phenolic hydroxyl group and the deshielding is due to hydrogen bonding with the solvent (remnants of water in the system).

The ^{1}H-NMR spectrum of A^2S to confirm the acetal dynamic exchange reaction after heating for 4 h at 110°C (above the Tv) indicating the thermally induced and catalyst-free dynamic reaction, following the mechanisms of transacetalization and acetal metathesis are demonstrated in Figure S3a–c.[30]

3.2 | Mechanical properties

Figure 5A depicts a typical brittle fracture for all the specimens studied here. As tabulated in Table S2 in Data S1, A^2S_20%_2 h showed the highest tensile strength of 75 MPa and Young's Modulus of 813.86 MPa among the other studied samples. Tensile strength and the Young's Modulus increased gradually from 59 to 75 MPa and 604 to 813 MPa, respectively when the hardener (A^2S) content was increased from 10% to 20%, respectively. In Table S2, the material's indentation resistance and the hardness of each sample were calculated and tabulated. As was noted, the highest value was represented by A^2S_20%_2 h in Figure 5B. The enhanced topology stiffness brought about by the increased Schiff base and acetal motif content is the reason for this gradual rise. However, a slight decrease in ultimate tensile strength (UTS) was observed when the content was increased to 30%, possibly as a result of steric hindrance and chain stiffness forming a tangled network.

A^2S_20%_2 h exhibited the highest tensile strength and Young's Modulus as it is the optimum composition where the surface stress does not exceed the rupture conditions to a limit owing to the crosslinking which allows it to be used in applications that require strong rigid epoxies as a replacement to traditional thermosets and addresses the issues of sustainability.

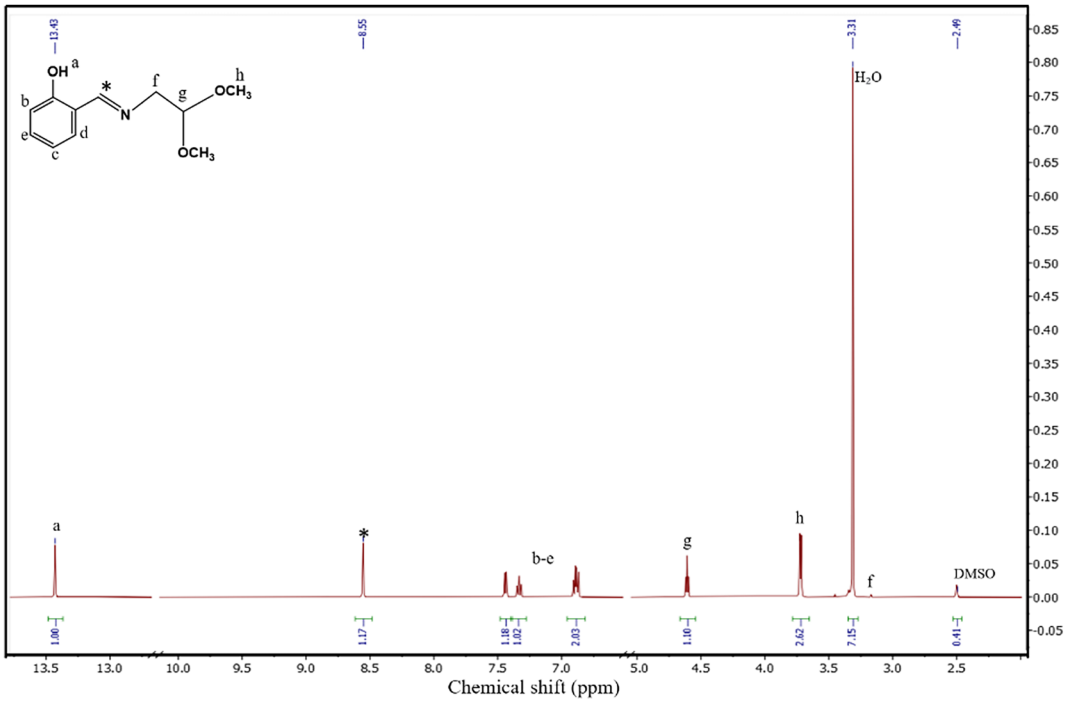

FIGURE 4 ^{1}H-NMR depicting the successful synthesis of (a) A^{2}S.

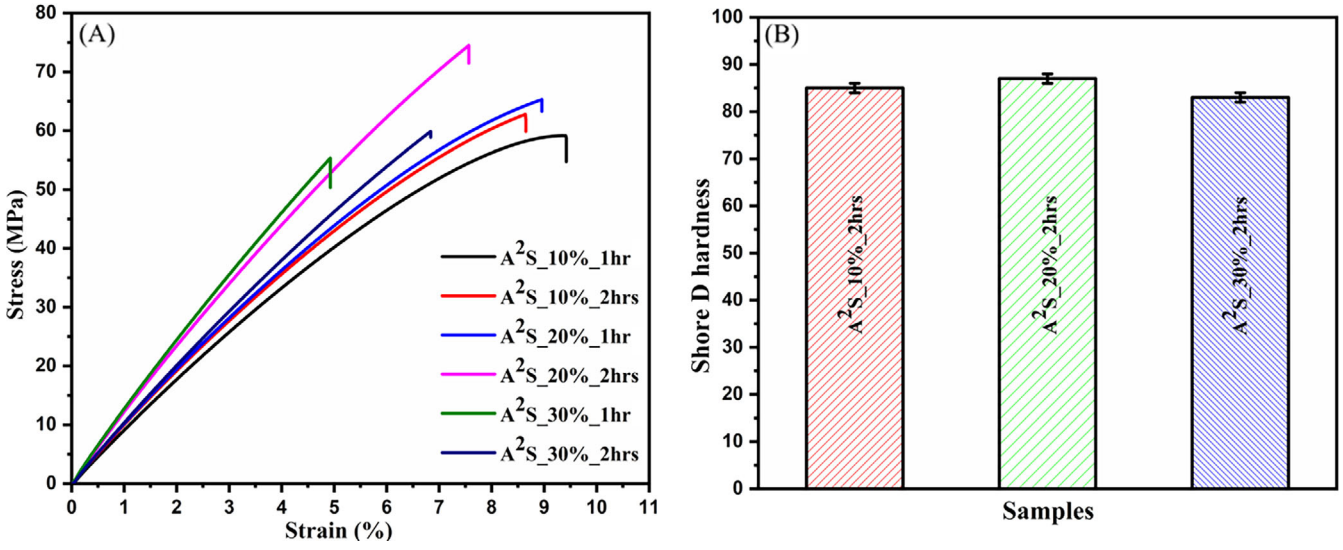

FIGURE 5 (A) Stress–strain curve; (B) Shore D hardness of all samples cured for 2 h.

3.3 | Thermal properties of the epoxy vitrimers

The transition temperature of the designed vitrimer was assessed using DSC isothermal heating rate (10°C/min). Based on the mechanical properties, as discussed above, A^{2}S_20% cured for 2 h showed the best properties and hence, the thermal properties were evaluated for this particular composition. The glass transition temperature of A^{2}S_20%_2 h was observed to be 121°C (see Figure 6A).

The transient network restricts the macromolecular mobility during curing and hence the samples cured at 120°C for 2 h were superior to those cured at 80°C, 100°C for similar time frames. The TGA profile (see Figure 6B) exhibits an onset degradation temperature of 276°C and $T_{d30\%}$ of 380°C indicating that the service life of the designed epoxy vitrimer is very similar to those of the traditional epoxies cured using permanent hardener. This low Tg as a result of low crosslinking density in the dual CAN allows reprocessing and shape reconfigurability

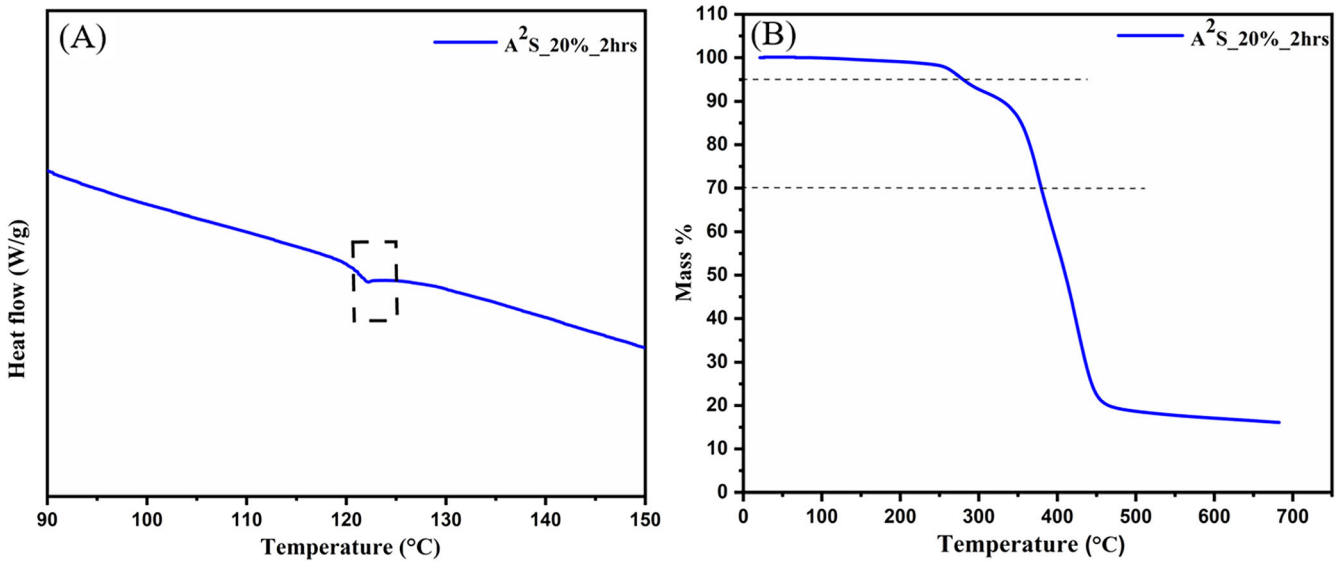

FIGURE 6 (A) DSC thermogram; (B) TGA analysis of SA-AACA-S-20-%.

behavior of vitrimers as it helps us determine the service temperature. This modified epoxy resin exhibited a high resistance to thermal degradation owing to the optimum crosslinking obtained in the system. Further, the thermal stability of the vitrimer was determined by the static heat-resistant index ($Ts = 255°C$) following the equation (3). The Ts was high in the case of dual CAN when compared with the one cured using traditional hardener ($Ts = 165°C$). This indicates that the vitrimer designed in this study can endure a temperature >200°C until there is no loss toward thermal degradation. This should be taken as an additional design parameter while designing dynamic hardener for epoxy-based systems. The higher heat resistant could also perhaps depend on the dynamic motif- here acetal. This also suggests that it might be beneficial in the preparation of heat-resistant products for container and storage applications.

$$T_s = 0.49[T_{d5\%} + 0.6(T_{d30\%} - T_{d5\%})]. \quad (3)$$

The dual dynamic hardener A^2S_20%_2 h developed facilitated the development of epoxy vitrimers with enhanced thermal resistance ($Ts = 255°C$) in comparison to traditional thermoset cured by employing permanent hardener to epoxy in the ratio of 1:9.

3.4 | DMA analysis: Flow activation energy and stress relaxation

The dynamic behavior was assessed for A2S_20%_2 h that showed superior mechanical strength and Shore D hardness among the different concentrations of A2S employed for curing epoxy at different curing times as discussed earlier. Figure 7A depicts storage modulus and tan δ as a function of temperature. The vitrimization process endowed in the system enables an exchange, reforming the network and this amalgamation and molecular segmental motions of the network occurring in the system results in increased storage modulus in the first stage (glassy region). The storage modulus eventually levels down with increased temperature as a consequence of the network formed with reduced molecular friction.[37]

According to the Maxwell model of a viscoelastic fluid, a typical relaxation time (τ) is the time at which E(t)/E0 decreases to 1/e, or ∼37%. The relaxation curves used to investigate the flow behavior of the developed polymer networks at various temperatures are depicted in Figure 7B and the flow activation energy exhibits a typical Arrhenius dependence of stress relaxation. The tan δ curve exhibits an area which depicts the material's ability to better absorb and dissipate energy and this further indicates a greater degree of molecular mobility in the system. This illustrates the capacity of the sample to infuse the developed systems with a dynamic exchange. The relaxation time (%) obtained for the sample as shown in Table 2 exhibits a gradual increase in relaxation rate as a function of temperature. The relaxation time (τ) for the sample decreased from 123.94 to 30.35 s as the temperature increased from 130 to 160°C. The rigid structure of DGEBA, which limits the mobility of the polymer chain, resulted in the sluggish relaxation of the sample at 130°C and as the temperature increases, there is rapid exchange of the dynamic networks. Moreover, the mobility of the molecular chains increases, thereby accelerating the rearrangement.[38,39]

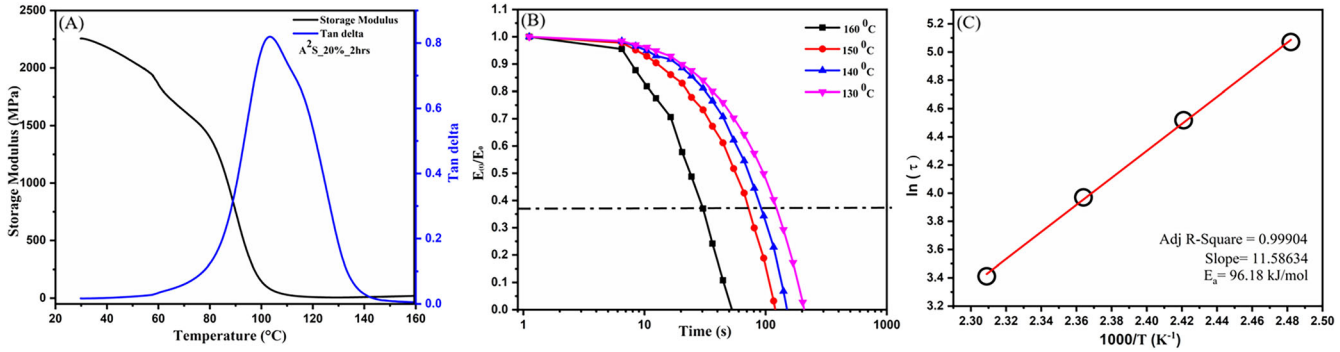

FIGURE 7 (A) Storage modulus and tan δ as a function of temperature; (B) Relaxation modulus versus time at different temperatures for samples; (C) Arrhenius plot of ln (τ) versus 1000/T of epoxy resin cured by A^2S_20%_2 h.

TABLE 2 Data obtained from DMA studies for sample A^2S_20%_2 h.

Sample	Storage Modulus (MPa)	Activation Energy (Ea. KJ/mol)	Stress relaxation time (s) 130°C	140°C	150°C	160°C	Tv (°C)
A^2**S**_20%_2 h	2260.52	96.18	123.94	80.12	54.12	30.35	105.5

The direct exchange of dynamic networks in the sample is temperature-dependent, and as a result, follows the characteristic Arrhenius behavior as defined by Equation 4.

$$\ln(\tau) = \ln(\tau_0) + \frac{E_a}{RT}, \quad (4)$$

where R is the universal gas constant, Ea is the bond exchange activation energy, T is the experiment temperature, and is the characteristic relaxation time. Figure 7C shows the linear relationship of ln(τ) against 1000/T, which yields the activation energy (Ea). The activation energy obtained for dual CAN (Ea = 96.18 kJ/mol) suggests that the dual dynamic networks integrated into the framework promote faster exchange. Leiber et al. in 2011 defined the topological freezing temperature (Tv), which is the temperature at which the internal dynamic linkages in a network appear to be frozen and are kinetically trapped.[4] At Tv, the network reorganizes as the materials transit from elastic to viscoelastic-liquid with viscosity approaching = 10^{12} Pas. The Tv for the system was calculated by extrapolating the fitted line using Equation (5), as shown in Table 2.

$$\eta = \tfrac{1}{3}E'\tau, \quad (5)$$

where, E' stands for the rubbery plateau from DMA.

The T_v obtained for the present system is 105°C, and is significantly lower than the Tg. This provides an explanation for the rapid relaxation seen for the sample at temperatures above Tg. The vitrimer can be reprocessed and recycled above Tv. Hence, along with determining the maximum temperature at which vitrimers can be used, it has a direct impact on the performance of the sample.[40]

Utilizing dynamic mechanical analysis, the crosslinking density (Vc) of the cured resins is determined to be the number of elastic functional groups per unit volume of the sample. Equation 6 is used to empirically determine Vc using the rubber elasticity hypothesis above Tg.[41]

$$V_C = \frac{E'}{3} \cdot A \cdot R \cdot T, \quad (6)$$

where, from the rubbery plateau, E′ is recorded at 30°C above Tg, A is the front factor, which is usually believed to be unity, R is the gas constant (8.314 J mol K^{-1}), and T is Tg DMA + 30 K.

The average molecular weight between the crosslinks is determined following equation 7.

$$M_c = d/V_C \quad (7)$$

where d is the cured resin's density. The samples exhibit a crosslinking density of 2211.04 mol$m^{-3}$and a M_c value of 526.44 g/mol.

The dual dynamic network showed crosslinking density and Vc which can be attributed to the molecular architecture of the dynamic hardener and the molecular makeup.[42] The elongation at break obtained for the vitrimer with dual CAN is low and the

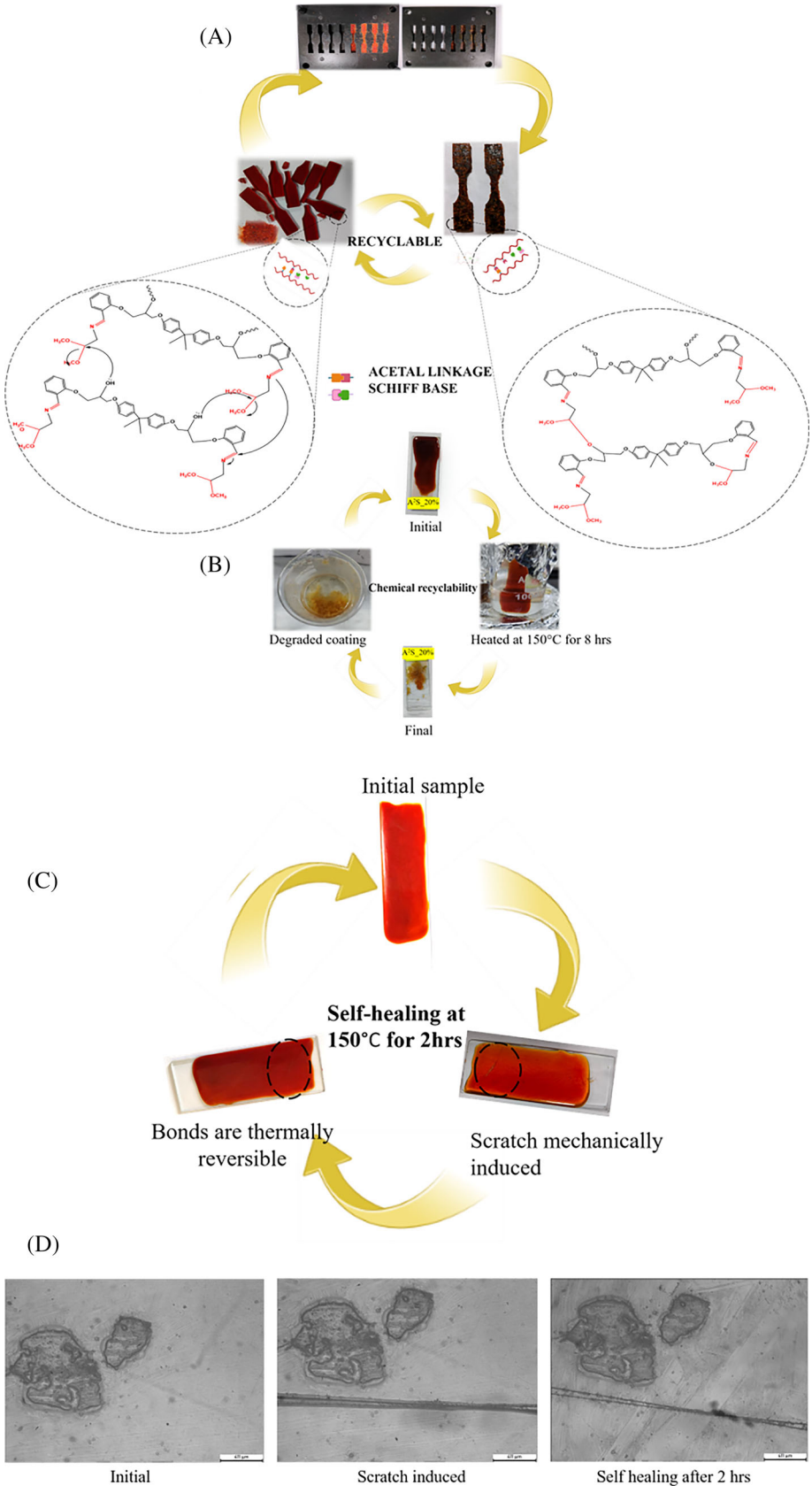

FIGURE 8 (A) Illustration of the mechanical recyclability of the samples by compression molding; (B) Chemical recyclability of the coating on glass substrate; (C) Self-healing of the vitrimer coating on metal substrate; (D) Optical microscopic images demonstrating healing.

extension ratio to break in elastomers is proportional to the square root of the reciprocal of the density of crosslinks[43] and vitrimers are elastic owing to the associative exchangeable crosslinks and this allows polymer circularity in the case of thermoset elastomers.[3] Similarly, the greater soluble fraction (tabulated in

Table S3) obtained in this study also provides a compelling argument that crosslinking can cut down the absorption and swelling in solvents and this emphasizes on the need for development of a system with optimum crosslinking density enough to provide good recyclability for the system designed.[44]

3.5 | Recyclability of vitrimer

Sustainability is a critical parameter in materials exploration, and vitrimer stand out because of their pliability and recyclability. The material's ability to reshape and heal itself contributes to its recyclability, thereby increasing its lifespan. Mechanical recyclability of the samples is demonstrated by grinding the samples to powder and remolding by compression molding as depicted in Figure 8A. Many applications need coatings with attributes like self-healing and re-generating ability. To show that the vitrimer designed here has the ability to re-cycle, we prepared a few glass substrates coated with A^2S. Post-curing, the glass substrates were immersed (Figure 8B) in 40 mL of 1 N HCl and THF (1:1) for 8 h at 100°C. The coating was dissolved following this treatment which manifests that these coatings are re-generative. Thermal healing endowed by the dual dynamic vitrimer demonstrated on glass substrate (Figure 8C) shows that complete healing can be obtained within 2 h at 150°C. This is also demonstrated by optical microscopy.

Bond breakage (imine and acetal) occurs at the molecular level during grinding. When heated, these thermoreversible linkages reunite, allowing the powder to flow and fuse on applying appropriate pressure and temperature. Hence, the recyclability is endowed by the inbuilt thermo-reversible acetal linkage and Schiff base.

3.6 | Degradation of A^2S cured epoxy

Due to their durability and high strength-to-weight ratio, high-performance carbon fiber reinforced composites (CFRCs) are utilized extensively in the aerospace and

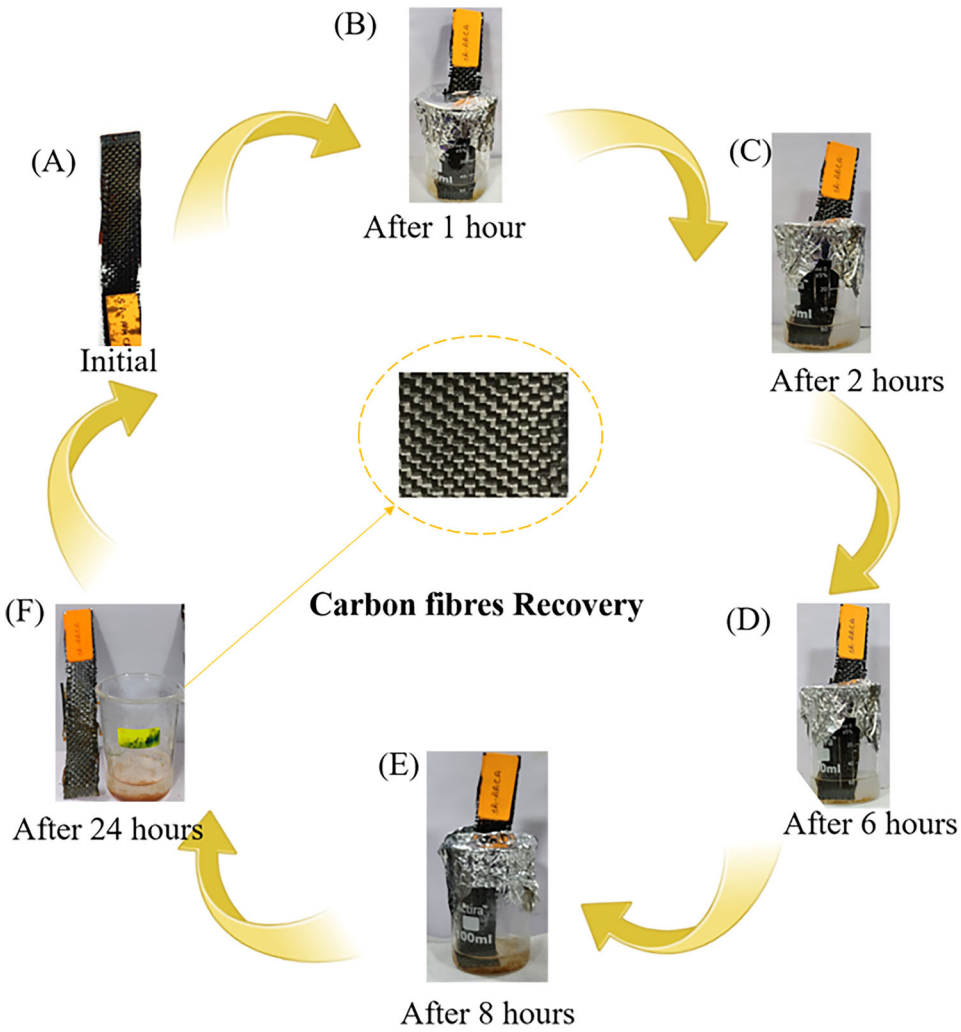

FIGURE 9 An illustration of recovery of fibers from A^2S_20% _2 h laminates samples at 100°C for 24 h.

ground transportation industries. However, environmental concerns have been raised as they are mostly not recycled. CFRCs are non-recyclable due to the presence of permanent crosslinks and the lengthy curing times required to create the polymeric network. The designed epoxy vitrimer ($A^2S\_20\%$) were hand-layed up on carbon fiber mat. By dissolving the matrix post-curing, the CF mat was successfully recovered (see Figure 9). As acetal and imine dynamic linkages can be hydrolysed into aldehydes, hydroxyl, and amine groups under mild acidic conditions, it can be degraded and the CF mat can be recovered.[45] The coating fragmented into smaller pieces, possibly because of the acetal network's de-crosslinking and if waited long enough, the coating would completely disintegrate. The degradation of traditional epoxy frameworks frequently requires high temperature and pressure however, in this case, the vitrimer can be degraded under mild acidic conditions and at relatively lower temperature and pressure.[46,47,45] Hence, our designed vitrimer can be a potential alternative in myriad applications.

The faster stress relaxations (30.35 s at 160°C) as obtained using DMA observed helps in rapid self-healing as depicted. The material is re-generative owing to the chemical solubility and degradation of the epoxy cured by the hardener in certain solvents and thus allows it to be used for the carbon fiber recovery.

4 | CONCLUSION

Conventional epoxies though offer myriad opportunities but suffer from lengthy curing cycles and after the useful life of the component, often end up in the landfill. By installing a dynamic hardener containing dual exchangeable bonds (here acetal and imine) the synthetic epoxy can be converted into a vitrimer which can switch between thermoset and thermoplastic controlled by the vitrimer transition temperature. The transient network aided by the dynamic hardener allows the vitrimer to cure within 2 h and displays excellent mechanical properties with a high tensile strength of up to 75 MPa and a glass transition temperature (Tg) of 121°C. It also exhibits fast stress relaxation, with a flow activation energy of 96.18 kJ/mol and relaxation time of 30 s at 160°C. The ability of the vitrimer to re-purpose or re-cycle was demonstrated by developing a laminate, through hand-layup, wherein the vitrimer was coated and cured using optimum processing conditions. Post-curing, the vitrimer was disintegrated, and the CF mat was recovered. Additionally, the final cured samples were re-shaped by hot pressing them above the transition temperature. The dynamic exchange installed in the vitrimer promoted self-healing as demonstrated in the coating applications. The unique network topology and exchangeable bonds make them attractive candidates for next-generation composites and laminates. This study provides a novel approach to recovering "smart" materials for sustainable and inexpensive technologies from classic thermoset recycling, utilizing commonly operated equipment and without the need to change the polymer processing industry's infrastructure. The development of vitrimer composites is continuing because of its multiple advantages such as reprocessability, reparability, and recyclability. This newfound interest brings up new green opportunities for the composite field, such as fracture treatment and molding defects. These new possibilities of incorporating vitrimers are frequently investigated on a small scale, and it will be interesting in the near future to demonstrate these capabilities on a much larger scale on composite parts or by healing the defects obtained during composite manufacturing. This will provide a crucial opportunity on the true industrial potential of vitrimer.

CONFLICT OF INTEREST STATEMENT

There is no conflict of interest.

DATA AVAILABILITY STATEMENT

Data has been peer reviewed.

ORCID

Suryasarathi Bose https://orcid.org/0000-0001-8043-9192

REFERENCES

1. Guerre M, Taplan C, Winne JM, Du Prez FE. Vitrimers: directing chemical reactivity to control material properties. *Chem Sci*. 2020;11(19):4855-4870. doi:10.1039/D0SC01069C
2. Alabiso W, Schlögl S. The impact of Vitrimers on the industry of the future: chemistry, properties and sustainable forward-looking applications. *Polymers (Basel)*. 2020;12(8):1. doi:10.3390/polym12081660
3. Luo J, Demchuk Z, Zhao X, et al. Elastic vitrimers: beyond thermoplastic and thermoset elastomers. *Matter*. 2022;5(5):1391-1422. doi:10.1016/j.matt.2022.04.007
4. Montarnal D, Capelot M, Tournilhac F, Leibler L. Silica-like malleable materials from permanent organic networks. *Science*. 2011;334(6058):965-968. doi:10.1126/science.1212648
5. Schenk V, Labastie K, Destarac M, Olivier P, Guerre M. Vitrimer composites: current status and future challenges. *Mater Adv*. 2022;3(22):8012-8029. doi:10.1039/D2MA00654E
6. Krishnakumar B, Sanka RVSP, Binder WH, Parthasarthy V, Rana S, Karak N. Vitrimers: associative dynamic covalent adaptive networks in thermoset polymers. *Chem Eng J*. 2020;385:123820. doi:10.1016/j.cej.2019.123820
7. Kloxin CJ, Scott TF, Adzima BJ, Bowman CN. Covalent adaptable networks (CANs): a unique paradigm in cross-linked

polymers. *Macromolecules*. 2010;43(6):2643-2653. doi:10.1021/ma902596s

8. Elling BR, Dichtel WR. Reprocessable cross-linked polymer networks: are associative exchange mechanisms desirable? *ACS Cent Sci*. 2020;6(9):1488-1496. doi:10.1021/acscentsci.0c00567
9. McBride MK, Worrell BT, Brown T, et al. Enabling applications of covalent adaptable networks. *Annu Rev Chem Biomol Eng*. 2019;10:175-198. doi:10.1146/annurev-chembioeng-060718-030217
10. Jourdain A, Asbai R, Anaya O, Chehimi MM, Drockenmuller E, Montarnal D. Rheological properties of covalent adaptable networks with 1,2,3-Triazolium cross-links: the missing link between vitrimers and dissociative networks. *Macromolecules*. 2020;53(6):1884-1900. doi:10.1021/acs.macromol.9b02204
11. Wu P, Liu L, Wu Z. A transesterification-based epoxy vitrimer synthesis enabled high crack self-healing efficiency to fibrous composites. *Compos Part A Appl Sci Manuf*. 2022;162:107170. doi:10.1016/j.compositesa.2022.107170
12. Bhusal S, Oh C, Kang Y, et al. Transesterification in Vitrimer polymers using Bifunctional catalysts: modeled with solution-phase Experimental rates and theoretical analysis of efficiency and mechanisms. *J Phys Chem B*. 2021;125(9):2411-2424. doi:10.1021/acs.jpcb.0c10403
13. Cuminet F, Berne D, Lemouzy S, et al. Catalyst-free transesterification vitrimers: activation via α-difluoroesters. *Polym Chem*. 2022;13(18):2651-2658. doi:10.1039/D2PY00124A
14. Miao P, Leng X, Liu J, Song G, He M, Li Y. Regulating the dynamic behaviors of Transcarbamoylation-based Vitrimers via mono-variation in density of exchangeable hydroxyl. *Macromolecules*. 2022;55(12):4956-4966. doi:10.1021/acs.macromol.2c00127
15. Denissen W, Rivero G, Nicolaÿ R, Leibler L, Winne J, Du Prez F. Vinylogous urethane vitrimers. *Adv Funct Mater*. 2015;25:25-2457. doi:10.1002/adfm.201404553
16. Spiesschaert Y, Danneels J, Van Herck N, et al. Polyaddition synthesis using alkyne esters for the design of Vinylogous urethane vitrimers. *Macromolecules*. 2021;54(17):7931-7942. doi:10.1021/acs.macromol.1c01049
17. Zych A, Tellers J, Bertolacci L, et al. Biobased, biodegradable, self-healing boronic ester vitrimers from epoxidized soybean oil acrylate. *ACS Appl Polym Mater*. 2021;3(2):1135-1144. doi:10.1021/acsapm.0c01335
18. Zhang X, Wang S, Jiang Z, Li Y, Jing X. Boronic Ester based Vitrimers with enhanced stability via internal boron-nitrogen coordination. *J Am Chem Soc*. 2020;142(52):21852-21860. doi:10.1021/jacs.0c10244
19. Tretbar CA, Neal JA, Guan Z. Direct silyl ether metathesis for vitrimers with exceptional thermal stability. *J Am Chem Soc*. 2019;141(42):16595-16599. doi:10.1021/jacs.9b08876
20. Wu S, Fang S, Tang Z, Liu F, Guo B. Bioinspired design of elastomeric vitrimers with sacrificial metal-ligand interactions leading to supramechanical robustness and retentive malleability. *Mater Des*. 2020;192:108756. doi:10.1016/j.matdes.2020.108756
21. Chen M, Zhou L, Wu Y, Zhao X, Zhang Y. Rapid stress relaxation and moderate temperature of malleability enabled by the synergy of disulfide metathesis and carboxylate transesterification in epoxy vitrimers. *ACS Macro Lett*. 2019;8(3):255-260. doi:10.1021/acsmacrolett.9b00015
22. Kuang X, Mu Q, Roach D, Qi H. Shape-programmable and healable materials and devices using thermo- and photo-responsive vitrimer. *Multifunct Mater*. 2020;3:45001. doi:10.1088/2399-7532/abbdc1
23. Guggari S, Magliozzi F, Malburet S, Graillot A, Destarac M, Guerre M. Vanillin-based epoxy Vitrimers: looking at the Cystamine hardener from a different perspective. *ACS Sustain Chem Eng*. 2023;11(15):6021-6031. doi:10.1021/acssuschemeng.3c00379
24. Memon H, Wei Y, Zhang L, Jiang Q, Liu W. An imine-containing epoxy vitrimer with versatile recyclability and its application in fully recyclable carbon fiber reinforced composites. *Compos Sci Technol*. 2020;199:108314. doi:10.1016/j.compscitech.2020.108314
25. Liu X, Zhang E, Feng Z, Liu J, Chen B, Liang L. Degradable bio-based epoxy vitrimers based on imine chemistry and their application in recyclable carbon fiber composites. *J Mater Sci*. 2021;56:1-19. doi:10.1007/s10853-021-06291-5
26. Memon H, Liu H, Abdur Rashid M, et al. Vanillin-based epoxy vitrimer with high performance and closed-loop recyclability. *Macromolecules*. 2020;53:53-630. doi:10.1021/acs.macromol.9b02006
27. Hendriks B, Waelkens J, Winne JM, Du Prez FE. Poly(thioether) vitrimers via transalkylation of trialkylsulfonium salts. *ACS Macro Lett*. 2017;6(9):930-934. doi:10.1021/acsmacrolett.7b00494
28. Li Q, Ma S, Wang S, et al. Facile catalyst-free synthesis, exchanging, and hydrolysis of an acetal motif for dynamic covalent networks. *J Mater Chem A*. 2019;7(30):18039-18049. doi:10.1039/C9TA04073K
29. Moreno A, Morsali M, Sipponen MH. Catalyst-free synthesis of lignin vitrimers with tunable mechanical properties: circular polymers and recoverable adhesives. *ACS Appl Mater Interfaces*. 2021;13(48):57952-57961. doi:10.1021/acsami.1c17412
30. Pemba A, Miller S. Acetal metathesis: mechanistic insight. *Synlett*. 2019;30:1971-1976. doi:10.1055/s-0037-1611833
31. Athawale A, Alhousami M. Epoxy resin-modified, Ureaformaldehyde/silicon networks for high impact strength and thermal stability. *J Reinf Plast Compos*. 2008;28:2231-2239. doi:10.1177/0731684408092366
32. El Gersifi K, Destais-Orvoën N, Durand G, Tersac G. Glycolysis of epoxide-amine hardened networks. I diglycidylether/aliphatic amines model networks. *Polymer (Guildf)*. 2003;44(14):3795-3801. doi:10.1016/S0032-3861(03)00324-0
33. Puglia D, Manfredi LB, Vazquez A, Kenny JM. Thermal degradation and fire resistance of epoxy–amine–phenolic blends. *Polym Degrad Stab*. 2001;73(3):521-527. doi:10.1016/S0141-3910(01)00157-4
34. Luo C, Wang W, Yang W, et al. High-strength and multi-recyclable epoxy Vitrimer containing dual-dynamic covalent bonds based on the disulfide and imine bond metathesis. *ACS Sustain Chem Eng*. 2023;11(39):14591-14600. doi:10.1021/acssuschemeng.3c04345
35. Xiang S, Zhou L, Chen R, Zhang K, Chen M. Interlocked covalent adaptable networks and composites relying on parallel connection of aromatic disulfide and aromatic imine cross-links in epoxy. *Macromolecules*. 2022;55(23):10276-10284. doi:10.1021/acs.macromol.2c01912

36. Ricciardi F, Joullié M, Romanchick W, Griscavage A. Mechanism of imidazole catalysis in the curing of epoxy resins. *J Polym Sci Polym Lett Ed*. 1982;20:127-133. doi:10.1002/pol.1982.130200209
37. Yue L, Guo H, Kennedy A, et al. Vitrimerization: converting thermoset polymers into Vitrimers. *ACS Macro Lett*. 2020;9(6):836-842. doi:10.1021/acsmacrolett.0c00299
38. Hao C, Liu T, Zhang S, Liu W, Shan Y, Zhang J. Triethanolamine-mediated covalent adaptable epoxy network: excellent mechanical properties, fast repairing, and easy recycling. *Macromolecules*. 2020;53(8):3110-3118. doi:10.1021/acs.macromol.9b02243
39. Hao C, Liu T, Zhang S, et al. A high lignin content removable and glycol-assisted repairable coating based on dynamic covalent bonds. *ChemSusChem*. 2018;12:12-1058. doi:10.1002/cssc.201802615
40. Yang Y, Zhang S, Zhang X, Gao L, Wei Y, Ji Y. Detecting topology freezing transition temperature of vitrimers by AIE luminogens. *Nat Commun*. 2019;10(1):3165. doi:10.1038/s41467-019-11144-6
41. Azcune I, Huegun A, ruiz de luzuriaga A, Saiz E, Rekondo A. The effect of matrix on shape properties of aromatic disulfide based epoxy vitrimers. *Eur Polym J*. 2021;148:110362. doi:10.1016/j.eurpolymj.2021.110362
42. Liu Y, Tang Z, Chen J, et al. Tuning the mechanical and dynamic properties of imine bond crosslinked elastomeric vitrimers by manipulating the crosslinking degree. *Polym Chem*. 2020;11(7):1348-1355. doi:10.1039/C9PY01826C
43. Taylor GR, Darin SR. The tensile strength of elastomers. *J Polym Sci*. 1955;17(86):511-525. doi:10.1002/pol.1955.120178604
44. Nielsen LE. Cross-linking–effect on physical properties of polymers. *J Macromol Sci Part C*. 1969;3(1):69-103. doi:10.1080/15583726908545897
45. Li Q, Ma S, Wang S, et al. Green and facile preparation of readily dual-recyclable thermosetting polymers with superior stability based on asymmetric Acetal. *Macromolecules*. 2020;53(4):1474-1485. doi:10.1021/acs.macromol.9b02386
46. Ma S, Wei J, Jia Z, et al. Readily recyclable, high-performance thermosetting materials based on a lignin-derived spiro diacetal trigger. *J Mater Chem A*. 2019;7(3):1233-1243. doi:10.1039/C8TA07140C
47. Li Q, Ma S, Li P, et al. Fast reprocessing of acetal covalent adaptable networks with high performance enabled by neighboring group participation. *Macromolecules*. 2021;54(18):8423-8434. doi:10.1021/acs.macromol.1c01046

SUPPORTING INFORMATION

Additional supporting information can be found online in the Supporting Information section at the end of this article.

How to cite this article: Tripathi S, H. S, Bose S. A designer Schiff based motif offered dual dynamic exchangeable bonds, faster curing and closed-loop circularity in epoxy vitrimers. *SPE Polym*. 2023; 1-15. doi:10.1002/pls2.10114